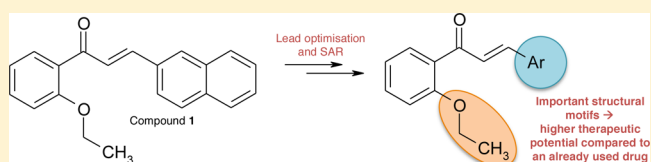


SAR-Guided Development and Characterization of a Potent Antitumor Compound toward B-Cell Neoplasms with No Detectable Cytotoxicity toward Healthy Cells

Gerda Brunhofer-Bolzer,^{†,‡} Trang Le,^{‡,§} Nils Dyckmanns,^{‡,§} Hanna A. Knaus,^{‡,§} Clemens Pausz,^{‡,§} Patricia Freund,^{‡,§} Ulrich Jäger,^{‡,§} Thomas Erker,^{*,†} and Katrina Vanura^{‡,§}[†]Department of Medicinal Chemistry, University of Vienna, Althanstrasse 14, 1090 Vienna, Austria[‡]Department of Medicine I, Division of Hematology and Hemostaseology, Medical University of Vienna, 1090 Vienna, Austria[§]Comprehensive Cancer Center, Medical University of Vienna, 1090 Vienna, Austria

ABSTRACT: Acute hematological diseases (leukemias and aggressive lymphomas) can be cured in approximately half of the patients, while the other patients die from their disease. Chronic leukemias and indolent lymphomas can be well controlled for years in most cases. However, the cure rate of these patients is low and the course of the disease is characterized by frequent recurrence. Therefore, novel agents

for monotherapies or combination therapies still need to be explored. The presented study describes the identification of the chalcone derivative **15** on different types of human malignant cells of the lymphoid and myeloid lineage. Further experiments performed with compound **15** on peripheral blood mononuclear cells (PBMCs) of chronic lymphocytic leukemia (CLL) patients clearly stated a higher cytotoxicity in PBMC from CLL patients compared to healthy donors (HD). The newly identified chalcone derivative **15** showed a higher therapeutic potential than fludarabine, a drug already in use in lymphoma treatment.



INTRODUCTION

Hematologic malignancies are a highly diverse group of cancers, which affect bone marrow, blood, and the lymph nodes. They rank just outside the top 10 list of cancers worldwide¹ and are expected to constitute 9% of cancers and to account for 9.4% of deaths from cancers in the U.S. in 2013.² Roughly 75% of these neoplasms are of lymphoid, and the rest is of myeloid origin, incidence rates being ~20 for lymphoid and ~7 for myeloid entities, respectively, per 100 000 persons per year in Western countries.^{2–5}

Among lymphoid malignancies, mature B-cell neoplasms not only constitute the largest proportion of diseases (52%)³ but also show the highest incidence rates in Europe, 19.14 per 100 000, with similar numbers reported from other Western countries,⁴ and are predominately diagnosed in elderly persons.³ Because of the diversity of these malignancies, biology and pathological characteristics are highly heterogeneous as are clinical presentation and behavior and, subsequently, therapeutic requirements. Conventional therapeutic regimens include chemotherapy, chemoimmunotherapy, and hematopoietic stem cell transplantation; experimental treatments comprise small and targeting molecules. Still, 30–50% of patients are resistant to treatment, progress rapidly, and die of their disease. Novel first line therapies are often very effective with response rates from 70% to 90%; however, many patients relapse or develop resistant disease. For these refractory patients and for patients characterized by particularly adverse factors, novel treatment opportunities need to be provided and novel, targeted therapies have to be explored.

One of the approaches for the development of novel anticancer drugs is the assessment of naturally occurring compounds for cancer therapy. In this study, we were focusing on the chalcone scaffold as a template for the structure–activity guided development of selective cytotoxic compounds toward B-cell neoplasms. Chemically, chalcones are biosynthetic precursors of flavonoids, and both natural as well as synthetic derivatives have shown biologic activity in cancer cells.^{6–10} Recent studies have shown that chalcone derivatives exhibit cytotoxic activity in different tumor cell lines including hematological malignancies. (*E*)- α -Benzylthiochalcones were able to significantly inhibit proliferation of K562, a BCR-ABL positive chronic myeloid leukemia cell line.¹¹ Nevertheless little is known about the mode of action of chalcone-based compounds. Their apoptosis inducing properties seemed to be mediated by interference in microtubule formation,^{12–20} inhibition of nuclear factor κ B (NF- κ B),²¹ and/or depletion of mitochondrial glutathione.⁸

In this contribution, a promising cytotoxic agent with specificity to neoplastic cells, in particular to hematological malignancies, was developed by using a lead structure optimization procedure in the B-cell lines MEC1, U-2940, and OCI-LY7. Considering the different biological characteristics and therapeutic responses of lymphoma, we continued to study the effect of the most interesting compound on six additional types of human lymphoma and leukemia cells of

Received: September 24, 2014

both the lymphoid and myeloid lineage (HL60, K562, CCRF, Jurkat, SU-DHL6, SU-DHL9). Studies of the effect of the identified hit on normal cells position this compound as a potent and novel candidate in the hunt for new antitumor agents.

RESULTS AND DISCUSSION

In an initial screening of an in-house library mainly based on naturally occurring scaffolds, e.g., curcumins, imidazoles, benzanilides, as well as chalcones, we have identified 3-(2-naphthyl)-1-(2-ethoxyphenyl)-2-propen-1-one (**1**) as a highly potent cytotoxic agent with IC_{50} values in the nanomolar range. As initial screening panel, we used the three cell lines MEC1 (chronic lymphocytic leukemia), U-2940 (diffuse large B-cell lymphoma), and OCI-LY7 (non-Hodgkin lymphoma) representing B-cell neoplasms.

Structurally seen, the small molecule compound **1** represents a typical chalcone scaffold. It is characterized by an orthoethoxy-substituted phenyl part as ring A and a 2-naphthyl moiety symbolizing ring B. The focus of the present study was to guide the systematic identification of a growth inhibitor with specificity to neoplastic cells, as cytotoxicity toward healthy cells is mostly associated with adverse effects, which can be related to morbidity and mortality of the patient.²² To discriminate in vitro between structural elements necessary for potent cytotoxicity toward tumor cells, which at the same time clearly show less activity on normal cells, the compounds were additionally tested on the murine bone marrow fibroblast cell line M2-10B4. This cell line is regularly used as feeder layer when cultured with patient cells, providing additional support and survival signals in particular in drug screens.²³

Beginning with compound **1** as lead, we first started with homologous variation of the 2-alkoxy substituent of ring A. In the second step we used a bioisosteric replacement strategy to optimize the ring B site of compound **1** (Figure 1). In the last set of compounds we focused on the substitution pattern of ring A with respect to the ethoxy group. The ortho, meta, and para congeners of the three most active compounds were generated and biologically investigated (Table 2). All the compounds were obtained by base-catalyzed reaction of the corresponding acetophenone with an appropriate benzaldehyde derivative (Claisen–Schmidt condensation) (Scheme 1).

Initially, compounds were biologically tested in six concentration steps (0.1, 1, 5, 10, 50, and 100 μM) using the CellTiter-Blue cell viability assay (Promega, Madison, WI, USA) and an incubation time of 48 h. In the case of a highly active compound ($IC_{50} < 1 \mu\text{M}$) the tested concentration range was shifted to 0.005, 0.01, 0.05, and 0.1 μM to define the IC_{50} more precisely. IC_{50} values were calculated from at least two independent experiments with three replicates each. In order to evaluate the biologic activity of the new compounds, cytotoxicity was compared to that of fludarabine, an already approved drug for the treatment of various B-cell malignancies. The cytotoxic potential (IC_{50}) of fludarabine was 42 μM in MEC1, 2.0 μM in U-2940, and 106 μM in OCI-LY7 cells, respectively. Differences in IC_{50} values for the different cell types can be explained by the biological and genetic particularities of each subtype of B-cell non-Hodgkin lymphoma.^{24–28}

First Optimization Step. We used compound **1** as lead structure to study the influence of the ortho ethoxy group with respect to the biological activity. We kept the 3-(2-naphthyl)-1-phenyl-2-propen-1-one backbone and started to systematically

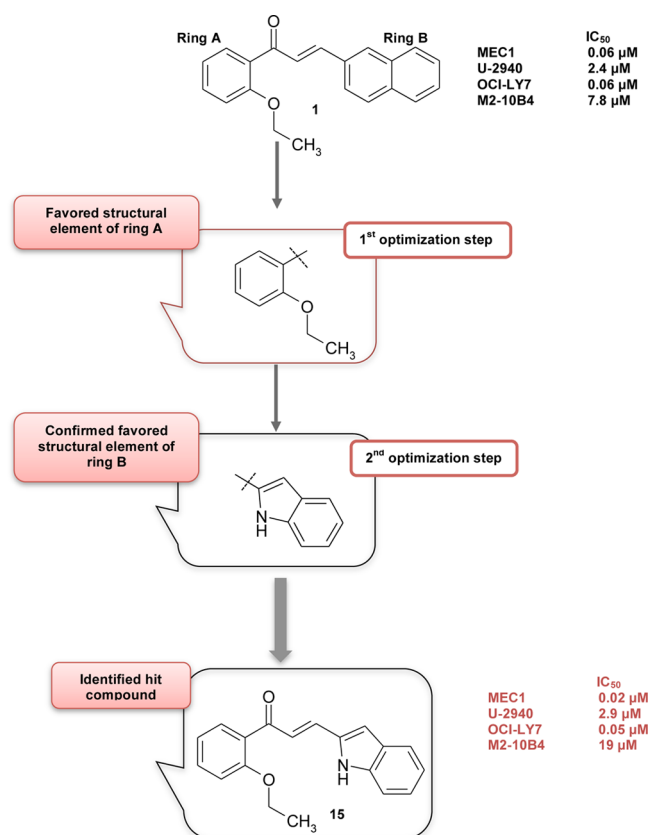
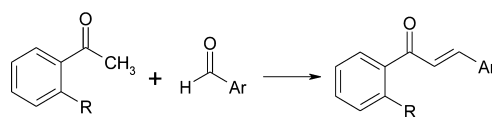


Figure 1. SAR studies based on the lead compounds **1** were obtained by structural modifications of ring A and ring B and resulted in compound **15** as new hit compound. Cytotoxic impact of compounds **1** and **15** on three malignant hematological cell lines (MEC1, U-2940, and OCI-LY7) as well as the mouse fibroblast cell line (M2-10B4) was used in the lead structure optimization process.

Scheme 1. Synthetic Route of Compounds 1–21^a

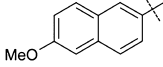
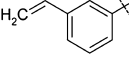
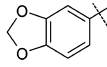
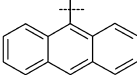
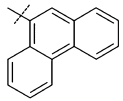
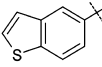
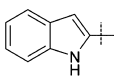


^aReagents and conditions: 50% NaOH, EtOH, room temp, 1–24 h.

vary the substituents of ring A in position 2. Hence, the first derivatives synthesized represented the homologous series of the alkoxy substituent and started by methoxy, followed by propoxy and butoxy. The biological data (Table 1) clearly showed the significance of this structural element: the methoxy derivative **2** demonstrated an almost 10-fold loss of activity on MEC1 and OCI-LY7 cells (0.43 and 0.46 μM) and half of the activity toward U-2940 (4.1 μM), although the unwanted cytotoxic potential on M2-10B4 ($IC_{50} = 42 \mu\text{M}$) was reduced. Elongation of the ethoxy group of compound **1** by one more methylene group to obtain the propoxy derivative **3** represented only half of the cytotoxic potency on the malignant kind of cell lines (0.13, 5.3, and 0.10 μM vs. 0.06, 2.4, and 0.06 μM). The compound did not show any activity on the mouse fibroblast cell line up to 100 μM . The inhibition of cell growth demonstrated clear SAR depending on the length of the alkoxy chain, as butoxy (compound **4**) showed reduced activity compared to the propoxy compound **3**. Compound **5** with an isopropoxy residue presented even weaker activity than

Table 1. Cytotoxic Activity of Compounds 1–15 on Three Malignant Hematological Cell Lines (MEC1, U-2940, and OCI-LY7) as Well as the Mouse Fibroblast Cell Line (M2-10B4)^b

1 st optimization step		IC ₅₀ (μM)			
Compound	R	MEC1	U-2940	OCI-LY7	M2-10B4
1 (Lead)	OC ₂ H ₅	0.06	2.4	0.06	7.8
2	OCH ₃	0.43	4.1	0.46	42
3	<i>O-propyl</i>	0.13	5.3	0.10	> 100
4	<i>O-butyl</i>	0.70	5.3	0.12	> 100
5		1.2	11	0.15	> 100
6	CH ₃	6.4	10	4.9	72

2 nd optimization step		IC ₅₀ (μM)			
Compound	Ar	MEC1	U-2940	OCI-LY7	M2-10B4
7		7.2	25	1.0	> 100
8		0.20	2.5	0.50	> 100
9		1.1	9.5	0.13	> 100
10		1.9	7.4	1.5	17
11		> 100	> 100	> 100	nt ^a
12		1.6	40	0.68	> 100
13		0.34	9.1	0.34	21
14		0.17	0.86	0.10	8.2
15		0.022	2.9	0.052	19

^ant: not tested

^ant: not tested. ^bFor comparison, IC₅₀ values (in μM) upon incubation with fludarabine, an approved drug for hematologic malignancies, were 42 (MEC1), 2.0 (U-2940), 105 (OCI-LY7), and >100 (M₂-10B4).

compounds 2 and 3. Moreover, by use of methyl instead of an alkoxy substituent as in the case in compound 6, the inhibitory activity on all three malignant cell lines decreased further to the lower micromolar range (6.4, 10, and 4.9 μM) and also a cytotoxic potential toward M2-10B4 was observed (72 μM). With regard to the biological activity, already small changes of the 2-substituent of ring A considerably influenced the inhibitory activity with ethoxy being the most favorable structural feature.

Second Optimization Step. As outlined above and demonstrated in Figure 1, the second optimization step focused on a bioisosteric replacement of ring B. The presence of a 6-methoxy substituent on the naphthyl part (compound 7) resulted in a cell line dependent loss of activity with no cytotoxic potential on M2-10B4 cells. Further modifications of the naphthyl moiety led to compound 8 with a “dissected” aromatic ring. The vinylphenyl derivative was almost equipotent in killing U-2940 cells (2.5 μM) but less active on

MEC1 and OCI-LY7 (0.20 and 0.50 μM) compared to compound 1 but did not show any activity on mouse fibroblasts. Further variations of ring B included a benzodioxole moiety (compound 9) as well as the 1-naphthyl congener of derivative 1, compound 10. Both modifications exhibited lower activity on MEC1 (1.1 and 1.9 μM), U-2940 (9.5 and 7.4 μM), and OCI-LY7 (0.13 and 1.5 μM). Compound 10 showed an IC₅₀ value of 17 μM on M2-10B4, which is about half as much as for compound 1 (7.8 μM). The insertion of a third phenyl ring led in the case of the anthracene derivative 11 to a complete loss of activity (up to 100 μM) toward all four cell lines, whereas with a phenanthrene moiety (compound 12) the cytotoxic activity on the malignant cell lines was retained even though it was a little bit lower compared to compound 1 (MEC1 1.6 μM, U-2940 40 μM, and OCI-LY7 0.68 μM). Introduction of 5- and 3-thionaphthene (compound 13 and 14), respectively, resulted in a 10-fold loss of cytotoxic activity in MEC1 and OCI-LY7 cells, whereas regarding U-2940 the 3-

thionaphthene (0.86 μM) proved to be more potent than its congener **13** (9.1 μM). This fact applies also for the healthy fibroblasts: compound **13** (21 μM) shows lower and compound **14** (8.2 μM) similar activity than the lead compound **1** (7.8 μM). In compound **15** the 2-naphthyl was replaced by a 2-indole ring system, which presented an improvement of the biological activity on the malignant cell lines (MEC 0.022 μM , U-2940 2.9 μM , and OCI-LY7 0.052 μM). Interestingly, the compound showed less cytotoxic potential on healthy cells (19 μM) in comparison to compound **1** (7.8 μM). Together, from steps 1 and 2 compound **15** resulted as a hit with respect to hematological B-cell malignancies.

Comparison of the Ortho, Meta, and Para Derivatives.

We systematically varied the position of the ethoxy group, which proved as biologically essential in the first optimization step. We have chosen compounds **1** (as original lead), **14**, and **15** (the two most active compounds arising from the optimization process) and synthesized and tested the corresponding congeners. Table 2 gives the obtained biological

Table 2. Comparison of the Biological Activity of the Meta (Position 3) and Para (Position 4) (MEC1, U-2940, and OCI-LY7)^a

Compound	Position of -OC ₂ H ₅	Ar	IC ₅₀ (μM)		
			MEC1	U-2940	OCI-LY7
1	2		0.06	2.4	0.060
16	3		2.9	16	1.8
17	4		nd	nd	nd
14	2		0.17	0.86	0.10
18	3		2.2	7.6	1.7
19	4		7.5	15	4.8
15	2		0.022	2.9	0.052
20	3		3.3	nd	4.8
21	4		>100	nd	25

^and: no significant cytotoxic activity was detected up to 100 μM .

results. In all three sets the meta and para isomers were 10- to 100-fold less active than the ortho isomer. It can be clearly seen that position 4 is being less preferred than position 3, which is very obvious in the case of the sets of compounds **1** and **15**. Therefore, the position of the ethoxy substituent plays an important role for the compounds' cytotoxic activity and ortho is proved to be the most favored pattern.

Together, compound **15** developed by two lead optimization processes turned out to have the optimal structural requirements for potent inhibition of malignant hematological cell lines with less biological activity on normal mouse fibroblasts. Especially in conjunction with chalcone derivatives, the 3,4,5-trimethoxyphenyl moiety is described as an essential structural feature of potent cytotoxic compounds.^{29–32} However, also in the case of other small molecules, for example, 1,5-diaryl-imidazole derivatives, this substitution pattern of the aromatic site proved to be the most favored.³³ In the hunt for specified cytotoxic compounds, we identified the 2-ethoxyphenyl part as a further highly active structural principle in the context of cytotoxic chalcone derivatives. Biological investigation of the homologous series of this structural feature proved the ethoxy substituent as most preferred. A recent study conducted by Maioral et al. investigating apoptosis induction of 1-naphthylchalcones in human acute leukemia cell lines described the derivative with a 2,5-dimethoxy substituent on the site of ring A as the most potent cytotoxic representative of the series tested with an IC₅₀ value of 40 μM on K562 and 21 μM on Jurkat cells after 24 h of incubation.³⁴ Moreover, the compound was shown to be nontoxic to peripheral blood lymphocytes with a cell viability of 99.89 \pm 10.69% at 50 μM compound concentration after 24 h. These data can be seen in accordance with the results obtained by the herein presented study: the 1-naphthylchalcone with a 2-methoxy substituent in ring A proved to be the most potent one. However, through optimization of both ring A and ring B we were able to obtain an even more potent cytotoxic compound on hematological cell lines.

Effect of Compound 15 on Other Hematological Cell Lines. As described above, hematologic malignancies are highly heterogeneous in their biology and behavior. This and the fact that some patient groups are resistant to therapy underline the

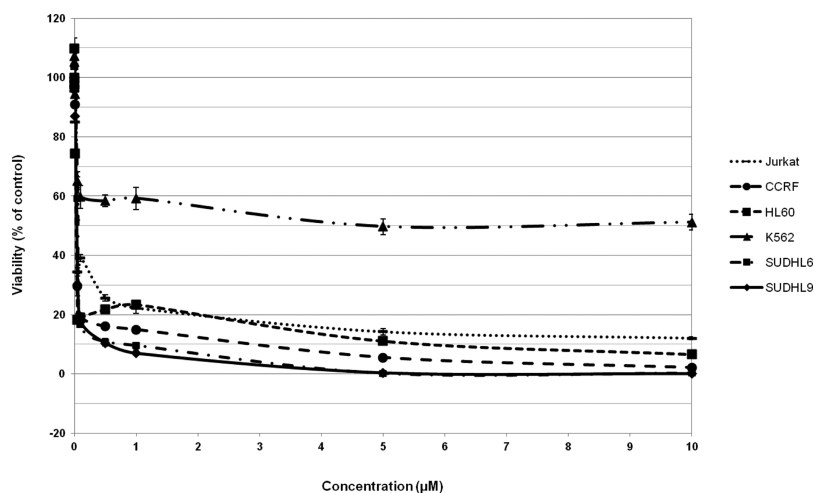


Figure 2. Cytotoxic effect of compound **15** on a variety of hematological cell lines. CCRF, Jurkat: T-cell acute lymphoblastic leukemia. HL60, K562: myeloid leukemia. SU-DHL6, SUDHL9: B-cell lymphoma. Viability was determined as described in the methods section and normalized to cells incubated with vehicle only. Mean values plus standard deviation are shown.

Table 3. IC₅₀ Values in μM Determined for Compound 15 in Different Cell Types^a

	CCRF	Jurkat	HL60	K562	SUDHL6	SUDHL9	CLL suspension	HD suspension	CLL coculture
15	0.032	0.038	0.016	n.d.	0.056	0.031	1.2	14	0.68
fludarabine	nd	nd	nd	nd	nd	nd	1.9	14	10

^aFor comparison, the standard therapeutic drug fludarabine was tested in parallel in experiments using primary cells. CCRF, Jurkat: T-cell acute leukemia. HL60, K562: myeloid leukemia. SU-DHL6, SU-DHL9: B-cell lymphoma. CLL suspension: primary CLL cells in suspension culture. HD suspension: healthy donor cells in suspension culture. CLL coculture: CLL cells in coculture with M2-10B4 fibroblast cells. nd: not determined.

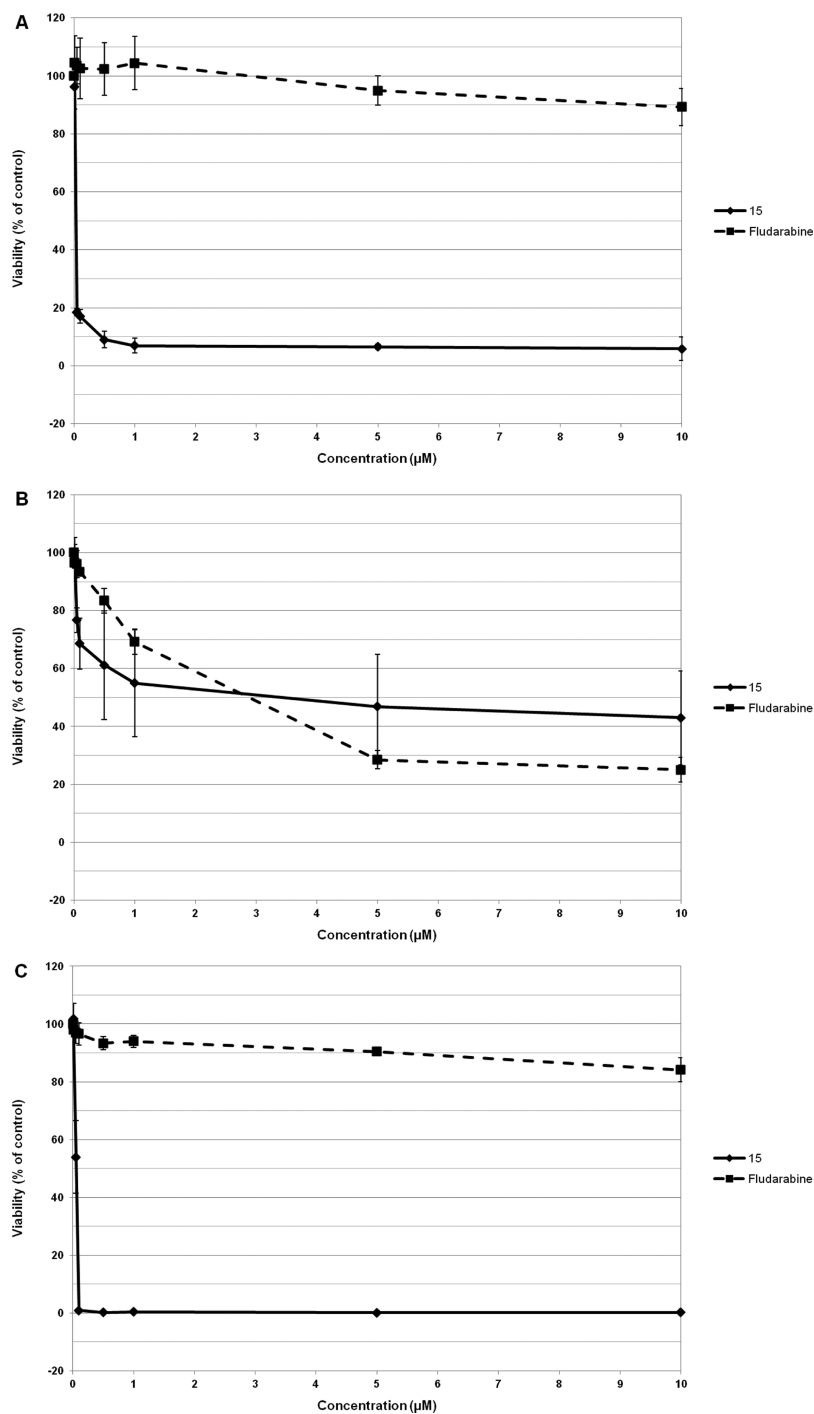


Figure 3. Comparing cytotoxic efficacies of compound 15 and fludarabine in three cell lines of the B-cell lineage: (A) MEC1; (B) U-2940; (C) OCI-LY7. Results were normalized to incubations with vehicle only. Mean values plus standard deviation are shown. IC₅₀ values (μM) were 0.022 and 42 (MEC1), 2.9 and 2.0 (U-2940), 0.052 and 106 (OCI-LY7) for compound 15 and fludarabine, respectively.

urgent need for new therapeutic drugs. Thus, after having developed compound 15 in our screening panel, we sought to

test this potent compound on other cell lines representing a variety of hematologic neoplasms: two T-cell acute leukemia

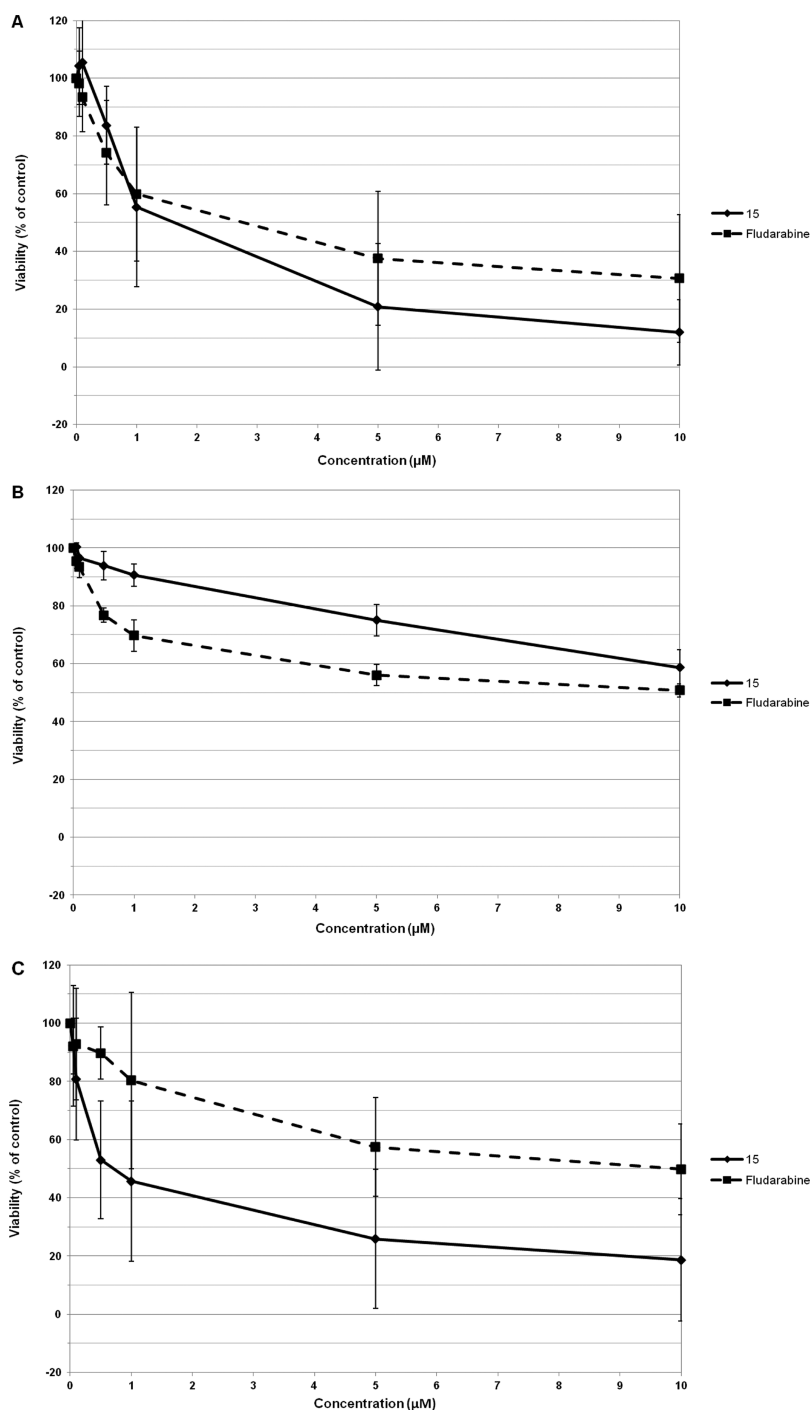


Figure 4. Comparison of cytotoxic efficacy of compound 15 and fludarabine in primary cells: (A) peripheral blood mononuclear cells (PBMCs) of chronic lymphocytic leukemia (CLL) patients ($N = 15$) tested in suspension culture; (B) PBMC of healthy individuals ($N = 4$) in suspension culture; (C) PBMC of CLL patients ($N = 9$) cultured over a layer of mouse fibroblast cells (M2-10B4). Results were normalized to incubations with vehicle only. Mean values plus standard deviation are shown. IC_{50} values are listed in Table 3.

cell lines (CCRF, Jurkat), two myeloid leukemia cell lines (HL60, K562), and two additional B-cell lines (SU-DHL6, SU-DHL9). Viability was assessed as described in the methods section; data are shown in Figure 2. Compound 15 considerably reduced the viability of cell lines to less than 30% of control already at concentrations of $<1 \mu\text{M}$. The exception was the chronic myeloid leukemia line K562. Although viability was reduced to 60% already at low concentrations, toxicity did not increase with increasing concentrations of compound 15 (Figure 2). However, this

cell line is derived from a patient in blast crisis and is characterized by a number of genetic aberrations associated with aggressive disease and resistance to treatment.³⁵ In all other cell lines, the biologic activity of compound 15 reached levels comparable to standard drugs used in therapy.^{36–42} IC_{50} values for compound 15 are listed in Table 3.

Comparison of Compound 15 with Fludarabine on MEC1, OCI-LY7, and U-2940. To put the efficacy of compound 15 into perspective, we screened the cell lines of our screening panel also with fludarabine. [(2R,3R,4S,5R)-5-(6-

Amino-2-fluoropurin-9-yl]-3,4-dihydroxyoxolan-2-yl]-methoxyphosphonic acid is a purine analogue that inhibits DNA synthesis through block of function of a number of enzymes required for DNA replication. It is used in combinations with rituximab, cyclophosphamide, dexamethasone, and mitoxantrone in various treatment regimens for indolent non-Hodgkin lymphomas. It also is part of the standard FCR therapy regimen for chronic lymphocytic leukemia (CLL) (fludarabine, cyclophosphamide, plus rituximab) as defined by the German CLL study group.⁴³ Although the function of compound **15** most likely is completely different compared to fludarabine, we decided to test the chalcone against a drug that right now may be considered as one of the standard chemotherapeutic agents in the treatment of hematologic malignancies.

As can be seen in Figure 3, compound **15** displayed much higher toxicity compared to fludarabine in MEC1 and OCI-LY7; furthermore it had comparable efficacy in U-2940 cells. This was also reflected in IC_{50} values, which were 1–3 log smaller for compound **15** compared to fludarabine (listed in Figure 3). Of note, while fludarabine had variable impact on viability in these three cell lines, the effect of compound **15** was more consistent. This not only reflects the biological and genetic differences involved but also suggests a high therapeutic potential of compound **15** in future antitumor regimens.^{24–26,28}

Investigating the Effect of Compound 15 in Primary Cells. As a last step, we wanted to evaluate cytotoxicity of compound **15** in primary cells and compare its activity to the impact of fludarabine. For this, peripheral blood mononuclear cells (PBMCs) of CLL patients were used in two experimental settings. They were cultured in conventional suspension culture being exposed to increasing concentrations of the tested compound. However, CLL cells need close contact with the tumor microenvironment depending on and receiving survival signals from stromal cells, which has impact on response to therapy. Therefore, as a second approach, CLL cells were cultured over a layer of mouse fibroblasts (M2-10B4) to include this biological aspect in drug evaluation. Such an approach is often used in preclinical assessment and testing of drugs in CLL cells.²³ Cells from healthy donors (HDs) were tested as control.

Figure 4 shows the reduction of viability in the tested settings, Table 3 lists the IC_{50} values for both compound **15** and fludarabine in CLL and HD primary cells. We observed higher cytotoxicity of compound **15** in PBMC from CLL compared to HD in suspension culture (Figure 4A and Figure 4B). Also, in comparison, fludarabine had less effect on tumor cells and displayed a greater reduction of viability in healthy cells. This indicates a more favorable therapeutic ratio for compound **15**. In coculture a protective effect for CLL cells usually is observed, as in our experiments with fludarabine (Figure 4C). In contrast, when incubated with compound **15**, CLL cells showed a reduction in viability comparable to that observed in suspension culture. Again, this indicates a high therapeutic potential of this novel compound.

EXPERIMENTAL SECTION

Chemistry. Unless stated otherwise, all chemicals were obtained from Sigma-Aldrich or Apollo Europe and were of analytical grade. Melting points were determined on a Kofler hot stage apparatus and are uncorrected. The 1H and ^{13}C NMR spectra were recorded on a BrukerAvance DPx200 (200 and 50 MHz). Chemical shifts are reported in δ units (ppm) relative to Me_4Si line as internal standard,

and J values are reported in hertz. Mass spectra were obtained by a Hewlett-Packard (GC, 5890; MS, 5970) spectrometer. The purity of the synthesized compounds was established by combustion analysis with a PerkinElmer 2400 CHN elemental analyzer and was within $\pm 0.4\%$. All biologically evaluated compounds were demonstrated to exist in $>95\%$ purity by CHN analysis. Solutions in organic solvents were dried over anhydrous sodium sulfate.

General Synthetic Procedure for Compounds 1–21. A solution of 2 mmol of the appropriate acetophenone derivative and 3 mL of 50% NaOH in 5 mL of ethanol was stirred at room temperature for 30 min. Then an amount of 2 mmol of the corresponding aldehyde derivative, dissolved in 3 mL of ethanol, was added and stirred at room temperature. After complete conversion of the starting materials (monitored by TLC), the reaction mixture was poured into ice-water or extracted with ethyl acetate. The organic layer was dried over anhydrous Na_2SO_4 and evaporated. The so-obtained crude product was purified by column chromatography or by recrystallization in ethanol.

3-(2-Naphthyl)-1-(2-ethoxyphenyl)-2-propen-1-one (1). Yield: 0.16 g (27%) yellow solid. Mp: 96–97 °C. 1H NMR ($CDCl_3$) δ 8.14–7.39 (m, 11H), 7.21–6.85 (m, 2H), 4.14 (q, J = 6.9 Hz, 2H), 1.43 (t, J = 6.9 Hz, 3H). ^{13}C NMR ($CDCl_3$) δ 192.7, 157.7, 142.6, 134.2, 133.4, 133.0, 132.8, 130.6, 130.3, 129.3, 128.6, 128.5, 127.7, 127.4, 127.1, 126.6, 123.6, 120.7, 112.6, 64.2, 14.8. MS m/z 302 (13%, M^+), 287 (2%), 273 (3%), 151 (77%), 68 (100%). Anal. Calcd for $C_{21}H_{18}O_2 \cdot 0.2H_2O$: C 82.44; H 6.06. Found: C 82.07; H 5.62.

1-(2-Methoxyphenyl)-3-(2-naphthyl)-2-propen-1-one (2). Yield: 0.35 g (60%) yellow solid. Mp: 81–83 °C. 1H NMR ($CDCl_3$) δ 7.96 (s, 1H), 7.91–7.70 (m, 5H), 7.65 (dd, J = 7.6 Hz, J = 1.6 Hz, 1H), 7.68–7.38 (m, 4H), 7.12–6.96 (m, 2H), 3.92 (s, 3H). ^{13}C NMR ($CDCl_3$): δ 193.0, 158.1, 143.4, 134.2, 133.3, 132.8, 132.6, 130.4, 130.3, 129.3, 128.6, 128.5, 127.8, 127.2, 127.2, 126.6, 123.7, 120.7, 111.6, 55.8. MS m/z 288 (61%, M^+), 287 (42%), 229 (39%), 152 (100%), 135 (47%). Anal. Calcd for $C_{20}H_{16}O_2$: C 83.31; H 5.59. Found: C 83.07; H 5.64.

3-(2-Naphthyl)-1-(2-propoxyphenyl)-2-propen-1-one (3). Yield: 0.42 g (66%) yellow oil. 1H NMR ($CDCl_3$) δ 7.96 (s, 1H), 7.89–7.65 (m, 6H), 7.65–7.39 (m, 4H), 7.09–6.93 (m, 2H), 4.02 (t, J = 6.4 Hz, 2H), 1.92–1.70 (m, 2H), 1.00 (t, J = 7.4 Hz, 3H). ^{13}C NMR ($CDCl_3$): δ 192.7, 157.8, 142.5, 134.2, 133.4, 133.0, 132.7, 130.6, 130.3, 129.4, 128.6, 128.5, 127.7, 127.5, 127.1, 126.6, 123.7, 120.6, 112.4, 70.1, 22.6, 10.7. MS m/z 316 (1%, M^+), 141 (9%), 85 (27%), 43 (100%), 41 (20%). Anal. Calcd for $C_{22}H_{20}O_2$: C 83.51; H 6.37. Found: C 83.11; H 6.09.

1-(2-Butoxyphenyl)-3-(2-naphthyl)-2-propen-1-one (4). Yield: 0.23 g (48%) yellow oil. 1H NMR ($CDCl_3$) δ 7.98 (s, 1H), 7.90–7.67 (m, 6H), 7.63 (s, 1H), 7.57–7.41 (m, 3H), 7.11–6.95 (m, 2H), 4.09 (t, J = 6.3 Hz, 2H), 1.88–1.70 (m, 2H), 1.59–1.38 (m, 2H), 0.87 (t, J = 7.3 Hz, 3H). ^{13}C NMR ($CDCl_3$) δ 192.7, 157.9, 142.5, 134.2, 133.4, 133.0, 132.8, 130.6, 130.3, 129.3, 128.6, 128.5, 127.8, 127.5, 127.1, 126.6, 123.7, 120.6, 112.4, 68.3, 31.3, 19.4, 13.7. MS m/z 330 (12%, M^+), 273 (38%), 189 (45%), 141 (100%), 121 (41%). Anal. Calcd for $C_{23}H_{22}O_2$: C 83.60; H 6.71. Found: C 83.17; H 6.49.

3-(2-Naphthyl)-1-[2-(2-propanoxy)phenyl]-2-propen-1-one (5). Yield: 0.48 g (76%) yellow solid. Mp: 82–85 °C. 1H NMR ($CDCl_3$) δ 7.98 (s, 1H), 7.91–7.40 (m, 10H), 7.09–6.96 (m, 2H), 4.66 (sept, J = 7.0 Hz, 1H), 1.37 (d, J = 7.0 Hz, 3H). ^{13}C NMR ($CDCl_3$) δ 192.9, 156.5, 142.2, 134.0, 133.3, 132.7, 130.6, 130.3, 130.2, 128.5, 128.4, 127.6, 127.4, 127.0, 126.5, 123.4, 120.6, 114.2, 71.0, 22.0. MS m/z 316 (25%, M^+), 273 (82%), 154 (100%), 152 (95%), 43 (39%). Anal. Calcd for $C_{22}H_{20}O_2 \cdot 0.3H_2O$: C 82.11; H 6.45. Found: C 82.05; H 6.33.

1-(2-Methylphenyl)-3-(2-naphthyl)-2-propen-1-one (6). Yield: 0.25 g (45%) yellow oil. 1H NMR ($CDCl_3$) δ 7.93 (s, 1H), 7.90–7.78 (m, 3H), 7.76–7.27 (m, 8H), 7.20 (s, 1H), 2.47 (s, 3H). ^{13}C NMR ($CDCl_3$) δ 197.0, 146.6, 139.6, 137.4, 134.8, 133.7, 132.6, 131.8, 131.1, 130.9, 129.2, 129.1, 128.5, 128.3, 127.9, 127.3, 127.2, 125.9, 124.0, 20.7. MS m/z 272 (30%, M^+), 141 (61%), 119 (100%),

91 (55%), 43 (37%). Anal. Calcd for C₂₀H₁₆O: C 88.20; H 5.92. Found: C 87.88; H 5.66.

1-(2-Ethoxyphenyl)-3-(6-methoxy-2-naphthyl)-2-propen-1-one (7). Yield: 0.46 g (68%) yellow solid. Mp: 97–99 °C. ¹H NMR (CDCl₃) δ 7.90 (s, 1H), 7.84–7.64 (m, 5H), 7.60–7.39 (m, 2H), 7.20–7.10 (m, 2H), 7.08–6.94 (m, 2H), 4.13 (q, J = 7.0 Hz, 2H), 3.92 (s, 3H), 1.43 (t, J = 7.0 Hz, 3H). ¹³C NMR (CDCl₃) δ 192.9, 158.8, 157.6, 143.1, 135.7, 132.9, 130.7, 130.5, 130.2, 130.1, 129.5, 128.8, 127.5, 126.5, 124.4, 120.7, 119.4, 112.6, 106.0, 64.3, 55.4, 14.9. MS *m/z* 332 (39%, M⁺), 171 (100%), 139 (65%), 121 (61%), 65 (35%). Anal. Calcd for C₂₂H₂₀O₃: C 79.50; H 6.06. Found: C 79.45; H 5.86

3-(3-Ethenylphenyl)-1-(2-ethoxyphenyl)-2-propen-1-one (8). Yield: 0.31 g (56%) yellow oil. ¹H NMR (CDCl₃) δ 7.72–7.24 (m, 8H), 7.08–6.91 (m, 2H), 6.74 (dd, J = 17.6 Hz, J = 10.8 Hz, 1H), 5.78 (dd, J = 17.6 Hz, J = 0.7 Hz, 1H), 5.29 (dd, J = 10.8 Hz, J = 0.7 Hz, 1H), 4.12 (q, J = 7.0 Hz, 2H), 1.42 (t, J = 7.0 Hz, 3H). ¹³C NMR (CDCl₃) δ 192.5, 157.6, 142.2, 138.1, 136.1, 135.4, 133.0, 130.5, 129.1, 129.0, 127.7, 127.4, 126.1, 120.6, 114.6, 112.5, 64.1, 14.8. MS *m/z* 278 (7%, M⁺), 161 (100%), 128 (36%), 121 (74%), 65 (23%). HRMS for C₁₉H₁₉O₂: 279.1385. Found: 279.1389

3-(1,3-Benzodioxol-5-yl)-1-(2-ethoxyphenyl)-2-propen-1-one (9). Yield: 0.29 g (49%) brown solid. Mp: 65–70 °C. ¹H NMR (CDCl₃) δ 7.69–7.27 (m, 4H), 7.13–6.92 (m, 4H), 6.86–6.77 (m, 1H), 6.00 (s, 2H), 4.13 (q, J = 7.0 Hz, 2H), 1.43 (t, J = 7.0 Hz, 3H). ¹³C NMR (CDCl₃) δ 192.6, 157.6, 149.5, 148.3, 142.5, 132.8, 130.5, 129.7, 129.5, 125.4, 124.8, 120.7, 112.6, 108.6, 106.5, 101.5, 64.2, 14.9. MS *m/z* 296 (4%, M⁺), 149 (19%), 135 (29%), 121 (25%), 43 (100%). Anal. Calcd for C₁₈H₁₆O₄·0.5H₂O: C 70.81; H 5.60. Found: C 70.82; H 5.35.

1-(2-Ethoxyphenyl)-3-(1-naphthyl)-2-propen-1-one (10). Yield: 0.47 g (78%) yellow solid. Mp: 109–110 °C. ¹H NMR (CDCl₃) δ 8.57–8.42 (m, 1H), 8.30–8.28 (m, 1H), 7.95–7.78 (m, 3H), 7.77–7.68 (m, 1H), 7.64–7.38 (m, 5H), 7.11–6.92 (m, 2H), 4.13 (q, J = 7.0 Hz, 2H), 1.42 (t, J = 7.0 Hz, 3H). ¹³C NMR (CDCl₃) δ 192.6, 157.7, 139.3, 133.7, 133.1, 132.6, 131.7, 130.7, 130.3, 129.7, 129.3, 128.7, 126.7, 126.2, 125.4, 124.9, 123.6, 120.7, 112.6, 64.2, 14.8. MS *m/z* 302 (40%, M⁺), 152 (88%), 141 (54%), 121 (98%), 43 (100%). Anal. Calcd for C₂₁H₁₈O₂·0.25Toluene: C 83.97; H 6.20. Found: C 84.00; H 5.82.

3-(9-Anthranil)-1-(2-ethoxyphenyl)-2-propen-1-one (11). Yield: 0.54 g (76%) yellow solid. Mp: 93–96 °C. ¹H NMR (CDCl₃) δ 8.66–8.51 (m, 1H), 8.44–8.25 (m, 3H), 8.05–7.91 (m, 2H), 7.81–7.72 (m, 1H), 7.55–7.34 (m, 6H), 7.12–6.99 (m, 1H), 6.98–6.88 (m, 1H), 4.08 (q, J = 6.9 Hz, 2H), 1.34 (t, J = 6.9 Hz, 3H). ¹³C NMR (CDCl₃) δ 192.5, 157.7, 139.7, 135.7, 133.2, 131.3, 130.7, 130.4, 129.5, 129.3, 128.8, 128.1, 126.1, 125.5, 125.3, 120.8, 112.4, 64.2, 14.8. MS *m/z* 352 (31%, M⁺), 202 (65%), 149 (61%), 121 (100%), 65 (21%). Anal. Calcd for C₂₅H₂₀O₂·0.14H₂O: C 84.60; H 5.76. Found: C 84.62; H 5.52.

1-(2-Ethoxyphenyl)-3-(9-phenanthrenyl)-2-propen-1-one (12). Yield: 0.38 g (54%) yellow solid. Mp: 117–120 °C. ¹H NMR (CDCl₃) δ 8.78–8.61 (m, 2H), 8.54–8.41 (m, 1H), 8.33–8.21 (m, 1H), 8.06 (s, 1H), 7.94–7.84 (m, 1H), 7.80–7.59 (m, 6H), 7.57–7.41 (m, 1H), 7.12–6.94 (m, 2H), 4.18 (q, J = 6.9 Hz, 2H), 1.48 (t, J = 6.9 Hz, 3H). ¹³C NMR (CDCl₃) δ 192.5, 157.8, 140.0, 133.2, 131.8, 131.2, 131.0, 130.7, 130.4, 130.3, 129.3, 129.1, 127.5, 127.0, 126.9, 126.4, 124.5, 123.1, 122.6, 120.8, 112.6, 64.3, 14.9. MS *m/z* 352 (49%, M⁺), 202 (83%), 191 (46%), 121 (100%), 57 (53%). Anal. Calcd for C₂₅H₂₀O₂: C 85.20; H 5.72. Found: C 85.05; H 5.44.

3-(5-Benzob[thienyl]-1-(2-ethoxyphenyl)-2-propen-1-one (13). Yield: 0.090 g (14%) yellow solid. Mp: 104–106 °C. ¹H NMR (CDCl₃) δ 8.03–7.97 (m, 1H), 7.94–7.33 (m, 8H), 7.10–6.94 (m, 2H), 4.15 (q, J = 7.0 Hz, 2H), 1.44 (t, J = 7.0 Hz, 3H). ¹³C NMR (CDCl₃) δ 192.8, 157.7, 142.9, 140.1, 132.9, 131.7, 130.6, 129.5, 127.5, 126.9, 124.6, 124.1, 123.2, 122.9, 120.7, 112.6, 64.3, 14.9. MS *m/z* 308 (11%, M⁺), 279 (14%), 161 (38%), 147 (100%), 121 (37%), 65 (21%). Anal. Calcd for C₁₉H₁₆O₂S·0.15H₂O: C 73.36; H 5.28. Found: C 73.44; H 4.95.

3-(1-Benzothien-3-yl)-1-(2-ethoxyphenyl)-2-propen-1-one (14). Yield: 0.39 g (63%) yellow oil. ¹H NMR (CDCl₃) δ 8.13–7.81

(m, 3H), 7.80–7.56 (m, 3H), 7.50–7.33 (m, 3H), 7.10–6.90 (m, 2H), 4.12 (q, J = 7.0 Hz, 2H), 1.41 (t, J = 7.0 Hz, 3H). ¹³C NMR (CDCl₃) δ 192.3, 157.7, 140.5, 137.3, 134.1, 133.1, 132.5, 130.7, 129.2, 128.3, 127.4, 125.0, 124.8, 122.9, 122.2, 120.7, 112.6, 64.2, 14.8. MS *m/z* 308 (43%, M⁺), 147 (100%), 121 (98%), 43 (89%), 41 (30%). Anal. Calcd for C₁₉H₁₆O₂S: C 74.00; H 5.23. Found: C 73.71; H 4.92.

1-(2-Ethoxyphenyl)-3-(1H-indole-2-yl)-2-propen-1-one (15). Yield: 0.22 g (38%) brown solid. Mp: 124–126 °C. ¹H NMR (CDCl₃) δ 9.05 (sbr, 1H), 7.72–7.54 (m, 3H), 7.49–6.89 (m, 7H), 6.87–6.80 (m, 1H), 4.08 (q, J = 7.0 Hz, 2H), 1.37 (t, J = 7.0 Hz, 3H). ¹³C NMR (CDCl₃) δ 192.9, 157.4, 138.0, 134.3, 133.3, 132.8, 130.3, 129.2, 128.5, 124.9, 124.5, 121.4, 120.6, 120.4, 112.6, 111.3, 108.8, 64.3, 14.7. MS *m/z* 291 (63%, M⁺), 262 (42%), 130 (61%), 119 (100%), 91 (49%). Anal. Calcd for C₁₉H₁₇NO₂: C 78.33; H 5.88; N 4.81. Found: C 78.24; H 5.67; N 4.79.

3-(2-Naphthyl)-1-(3-ethoxyphenyl)-2-propen-1-one (16). Yield: 0.21 g (34%) yellow solid. Mp: 97–100 °C. ¹H NMR (CDCl₃) δ 8.03–7.76 (m, 6H), 7.66–6.37 (m, 6H), 7.15–7.05 (m, 1H), 4.12 (q, J = 7.0 Hz, 2H), 1.45 (t, J = 7.0 Hz, 3H). ¹³C NMR (CDCl₃) δ 190.4, 159.4, 145.0, 139.8, 134.6, 133.5, 132.6, 130.8, 129.8, 128.9, 128.8, 128.0, 127.5, 126.9, 123.9, 122.4, 121.1, 119.8, 113.8, 63.9, 15.0. MS *m/z* 302 (100%, M⁺), 181 (36%), 152 (84%), 128 (18%), 65 (15%). Anal. Calcd for C₂₁H₁₈O₂: C 83.42; H 6.00. Found: C 83.12; H 5.95.

3-(2-Naphthyl)-1-(4-ethoxyphenyl)-2-propen-1-one (17). Yield: 0.44 g (73%) yellow solid. Mp: 159–161 °C. ¹H NMR (CDCl₃) δ 8.09–7.48 (m, 11H), 6.97 (d, J = 8.8 Hz, 2H), 4.11 (q, J = 7.0 Hz, 2H), 1.45 (t, J = 7.0 Hz, 3H). ¹³C NMR (CDCl₃) δ 188.8, 163.0, 144.1, 134.4, 133.5, 132.8, 131.1, 131.0, 130.6, 128.8, 128.8, 127.9, 127.4, 126.9, 123.9, 122.2, 114.5, 63.9, 14.9. MS *m/z* 302 (99%, M⁺), 273 (36%), 152 (100%), 121 (59%), 65 (37%). Anal. Calcd for C₂₁H₁₈O₂: C 83.42; H 6.00. Found: C 83.07; H 5.87.

3-(1-Benzothien-3-yl)-1-(3-ethoxyphenyl)-2-propen-1-one (18). Yield: 0.21 g (34%) yellow solid. Mp: 103–106 °C. ¹H NMR (CDCl₃) δ 8.15–8.07 (m, 2H), 7.92–7.88 (m, 2H), 7.65–7.38 (m, 6H), 7.16–7.11 (m, 1H), 4.12 (q, J = 7.0 Hz, 2H), 1.45 (t, J = 7.0 Hz, 3H). ¹³C NMR (CDCl₃) δ 190.3, 159.5, 140.7, 139.7, 137.5, 136.5, 132.5, 129.8, 128.9, 125.3, 125.2, 123.3, 122.7, 122.4, 121.0, 119.9, 113.8, 63.9, 15.0. MS *m/z* 308 (60%, M⁺), 279 (26%), 187 (48%), 115 (100%), 69 (56%). Anal. Calcd for C₁₉H₁₆O₂S: C 74.00; H 5.23. Found: C 73.99; H 4.87.

3-(1-Benzothien-3-yl)-1-(3-ethoxyphenyl)-2-propen-1-one (19). Yield: 0.45 g (74%) yellow solid. Mp: 129–130 °C. ¹H NMR (CDCl₃) δ 8.14–8.04 (m, 4H), 7.92–7.88 (m, 2H), 7.65 (AB-system, J_{AB} = 15.6 Hz, 1H), 7.50–7.41 (m, 2H), 7.00–6.96 (m, 2H), 4.12 (q, J = 7.0 Hz, 2H), 1.46 (t, J = 7.0 Hz, 3H). ¹³C NMR (CDCl₃) δ 188.7, 163.1, 140.7, 137.6, 132.7, 131.1, 131.0, 128.3, 125.3, 125.2, 123.2, 122.5, 122.4, 114.5, 64.0, 14.9. MS *m/z* 308 (100%, M⁺), 279 (27%), 251 (25%), 115 (35%), 65 (10%). Anal. Calcd for C₁₉H₁₆O₂S·0.13H₂O: C 73.44; H 5.27. Found: C 73.24; H 4.87.

1-(3-Ethoxyphenyl)-3-(1H-indole-2-yl)-2-propen-1-one (20). Yield: 0.18 g (31%) brown solid. Mp: 156–158 °C. ¹H NMR (CDCl₃) δ 8.99 (s, 1H), 7.85 (d, J = 15.6 Hz, 1H), 7.65–7.07 (m, 9H), 6.91 (s, 1H), 4.03 (q, J = 7.0 Hz, 2H), 1.40 (t, J = 7.0 Hz, 3H). ¹³C NMR (CDCl₃) δ 190.3, 159.4, 139.7, 135.0, 134.3, 129.8, 128.7, 125.1, 121.9, 121.0, 120.9, 119.9, 119.6, 113.7, 111.5, 110.3, 63.9, 14.9. MS *m/z* 291 (100%, M⁺), 262 (71%), 234 (49%), 170 (35%), 115 (32%). Anal. Calcd for C₁₉H₁₇NO₂: C 78.33; H 5.88. Found: C 78.20; H 5.56.

1-(4-Ethoxyphenyl)-3-(1H-indole-2-yl)-2-propen-1-one (21). Yield: 0.09 g (15%) brown solid. Mp: 178–181 °C. ¹H NMR (CDCl₃) δ 8.83 (sbr, 1H), 8.03–6.90 (m, 11H), 4.07 (q, J = 7.0 Hz, 2H), 1.43 (t, J = 7.0 Hz, 3H). ¹³C NMR (CDCl₃) δ 188.5, 163.1, 138.1, 134.0, 131.0, 130.9, 128.8, 125.0, 121.8, 120.9, 119.5, 114.5, 111.4, 109.8, 64.0, 14.9. MS *m/z* 291 (100%, M⁺), 262 (43%), 234 (29%), 117 (44%), 65 (30%). Anal. Calcd for C₁₉H₁₇NO₂: C 78.33; H 5.88, N 4.81. Found: C 78.18; H 5.40, N 4.77.

Cell Lines and Patients. Hematological cell lines were acquired from the Leibniz Institute DSMZ-German Collection of Microorganisms and Cell Cultures (www.dsmz.de) and the American Type Culture Collection (<http://www.lgcstandards-atcc.org/>). Sixteen

patients diagnosed with chronic lymphocytic leukemia at the Division of Hematology and Hemostaseology at the Vienna General Hospital and four healthy donors were included in the study. All participants signed informed consent according to the Declaration of Helsinki (Ethics Committee No. EK 1722/2012). Peripheral blood mononuclear cells (PBMCs) were isolated using standardized Ficoll–Hypaque gradient centrifugation (Seromed, Berlin, Germany) and stored in liquid nitrogen until use.

Cell Culture. JURKAT and CCRF-CEM (T-cell acute lymphoblastic leukemia), HL60 and K562 representing acute and chronic myeloid leukemia, respectively, the chronic lymphocytic leukemia cell line MEC1, and the diffuse large B-cell lymphoma cell line U-2940 were cultured in Gibco RPMI 1640 + GlutaMAX (Life Technologies, Carlsbad, CA, USA) containing phenol red and supplemented with 10% fetal bovine serum gold (FBS gold; PAA Laboratories, Pasching, Austria) and 1% PenStrep (100 U/mL penicillin and 100 µg/mL streptomycin; PAA Laboratories) and maintained at 37 °C in humidified atmosphere with 5% CO₂. The diffuse large B-cell lymphoma cell line OCI-LY7 was cultured in Gibco IMDM + GlutaMAX and 25 mM HEPES (Life Technologies, Carlsbad, CA, USA) containing phenol red and 20% FBS gold and 1% PenStrep.

Primary Cells. Primary cells were thawed in phenol red-free Gibco RPMI 1640 + L-glutamine (Life Technologies, Carlsbad, CA, USA) supplemented with 20% FBS gold and cultured overnight at standard conditions before cells were incubated with the compounds.

Viability Tests. All experiments with hematological cell lines were done using phenol red-free Gibco RPMI 1640 + L-glutamine supplemented with 1% PenStrep and 10% FBS gold except experiments with OCI-LY7 which were carried out in Gibco IMEM + GlutaMAX and 25 mM HEPES containing phenol red, 20% FBS gold, and 1% PenStrep. Cells were incubated in triplicates with increasing concentrations of the compounds for 48 h. Changes in viability were determined using the CellTiter-Blue cell viability assay (Promega, Madison, WI, USA) following instructions of the manufacturer. IC₅₀ values were calculated from two independent experiments using GraphPad Prism5 software.

Primary cells were incubated at a density of 300 000 cells per well in 96-well plates in a total volume of 100 µL of phenol red-free Gibco RPMI 1640 + L-glutamine supplemented with 20% FBS gold with increasing concentrations of compounds for 48 h. For coculture experiments, 150 000 M2-10B4 mouse fibroblast cells were seeded into 12-well plates and allowed to form a confluent layer overnight. Supernatant was replaced by 3 million primary cells in a total volume of 1 mL of medium and incubated with increasing concentrations of compounds for 48 h. Viability was measured as described above. Experiments with primary cells were done in triplicate. IC₅₀ values were calculated from the mean values of all samples used in the various experiments using GraphPad Prism5 software.

AUTHOR INFORMATION

Corresponding Author

*Phone: +43 (0)1 4277 55003. Fax: +43 (0)1 4277 95514. E-mail: thomas.erker@univie.ac.at.

Author Contributions

The manuscript was written through contributions of all authors. All authors have given approval to the final version of the manuscript.

Notes

The authors declare no competing financial interest.

ACKNOWLEDGMENTS

This work was supported by Joint Research Cluster of the University of Vienna and Medical University of Vienna “Platform for Accelerated Drug Optimization in Malignant Disease (PADO)” <http://forschungscluster.meduniwien.ac.at/pado/?L=0>.

ABBREVIATIONS USED

CCR2, CC chemokine receptor 2; CCL2, CC chemokine ligand 2; CCR5, CC chemokine receptor 5; TLC, thin layer chromatography

REFERENCES

- (1) World Health Organization. GLOBOCAN 2012. <http://globocan.iarc.fr/>.
- (2) *Facts 2013*; Leukemia & Lymphoma Society; White Plains, NY, 2013.
- (3) Jayasekara, H.; Karahalios, A.; Juneja, S.; Thursfield, V.; Farrugia, H.; English, D. R.; Giles, G. G. Incidence and survival of lymphohematopoietic neoplasms according to the World Health Organization classification: a population-based study from the Victorian Cancer Registry in Australia. *Leuk. Lymphoma* **2010**, *51*, 456–468.
- (4) Sant, M.; Allemani, C.; Tereanu, C.; De Angelis, R.; Capocaccia, R.; Visser, O.; Marcos-Gragera, R.; Maynadie, M.; Simonetti, A.; Lutz, J. M.; Berrino, F. Incidence of hematologic malignancies in Europe by morphologic subtype: results of the HAEMACARE project. *Blood* **2010**, *116*, 3724–3734.
- (5) *Cancer Facts & Figures 2013*; American Cancer Society: Atlanta, GA, 2013.
- (6) Henmi, K.; Hiwatashi, Y.; Hikita, E.; Toyama, N.; Hirano, T. Methoxy- and fluoro-chalcone derivatives arrest cell cycle progression and induce apoptosis in human melanoma cell A375. *Biol. Pharm. Bull.* **2009**, *32*, 1109–1113.
- (7) Kong, Y.; Wang, K.; Edler, M. C.; Hamel, E.; Mooberry, S. L.; Paige, M. A.; Brown, M. L. A boronic acid chalcone analog of combretastatin A-4 as a potent anti-proliferation agent. *Bioorg. Med. Chem.* **2010**, *18*, 971–977.
- (8) Navarini, A. L. F.; Chiaradia, L. D.; Mascarello, A.; Fritzen, M.; Nunes, R. J.; Yunes, R. A.; Creczynski-Pasa, T. B. Hydroxychalcones induce apoptosis in B16-F10 melanoma cells via GSH and ATP depletion. *Eur. J. Med. Chem.* **2009**, *44*, 1630–1637.
- (9) Yang, X.; Wang, W.; Tan, J.; Song, D.; Li, M.; Liu, D.; Jing, Y.; Zhao, L. Synthesis of a series of novel dihydroartemisinin derivatives containing a substituted chalcone with greater cytotoxic effects in leukemia cells. *Bioorg. Med. Chem. Lett.* **2009**, *19*, 4385–4388.
- (10) Szliszka, E.; Czuba, Z.; Mazur, B.; Sedek, L.; Paradysz, A.; Krol, W. Chalcones enhance TRAIL-induced apoptosis in prostate cancer cells. *Int. J. Mol. Sci.* **2009**, *11*, 1–13.
- (11) Reddy, M. V. R.; Pallela, V. R.; Cosenza, S. C.; Mallireddigari, M. R.; Patti, R.; Bonagura, M.; Truongcao, M.; Akula, B.; Jatiani, S. S.; Reddy, E. P. Design, synthesis and evaluation of (E)-[alpha]-benzylthio chalcones as novel inhibitors of BCR-ABL kinase. *Bioorg. Med. Chem.* **2010**, *18*, 2317–2326.
- (12) Bhat, B. A.; Dhar, K. L.; Puri, S. C.; Saxena, A. K.; Shanmugavel, M.; Qazi, G. N. Synthesis and biological evaluation of chalcones and their derived pyrazoles as potential cytotoxic agents. *Bioorg. Med. Chem. Lett.* **2005**, *15*, 3177–3180.
- (13) Ducki, S.; Forrest, R.; Hadfield, J. A.; Kendall, A.; Lawrence, N. J.; McGown, A. T.; Rennison, D. Potent antimitotic and cell growth inhibitory properties of substituted chalcones. *Bioorg. Med. Chem. Lett.* **1998**, *8*, 1051–1056.
- (14) Ducki, S.; Rennison, D.; Woo, M.; Kendall, A.; Chabert, J. F. D.; McGown, A. T.; Lawrence, N. J. Combretastatin-like chalcones as inhibitors of microtubule polymerization. Part 1: Synthesis and biological evaluation of antivascular activity. *Bioorg. Med. Chem.* **2009**, *17*, 7698–7710.
- (15) Edwards, M. L.; Stemerick, D. M.; Sunkara, P. S. Chalcones: a new class of antimitotic agents. *J. Med. Chem.* **1990**, *33*, 1948–1954.
- (16) Hsu, Y. L.; Kuo, P. L.; Tzeng, W. S.; Lin, C. C. Chalcone inhibits the proliferation of human breast cancer cell by blocking cell cycle progression and inducing apoptosis. *Food Chem. Toxicol.* **2006**, *44*, 704–713.

- (17) Lawrence, N. J.; Patterson, R. P.; Ooi, L.-L.; Cook, D.; Ducki, S. Effects of [alpha]-substitutions on structure and biological activity of anticancer chalcones. *Bioorg. Med. Chem. Lett.* **2006**, *16*, 5844–5848.
- (18) Liu, X.; Go, M.-L. Antiproliferative properties of piperidinyl-chalcones. *Bioorg. Med. Chem.* **2006**, *14*, 153–163.
- (19) Peyrot, V.; Leynadier, D.; Sarrazin, M.; Briand, C.; Rodriguez, A.; Nieto, J. M.; Andreu, J. M. Interaction of tubulin and cellular microtubules with the new antitumor drug MDL 27048. A powerful and reversible microtubule inhibitor. *J. Biol. Chem.* **1989**, *264*, 21296–21301.
- (20) Tu, H.-Y.; Huang, A. M.; Hour, T.-C.; Yang, S.-C.; Pu, Y.-S.; Lin, C.-N. Synthesis and biological evaluation of 2',5'-dimethoxychalcone derivatives as microtubule-targeted anticancer agents. *Bioorg. Med. Chem.* **2010**, *18*, 2089–2098.
- (21) Srinivasan, B.; Johnson, T. E.; Lad, R.; Xing, C. Structure–activity relationship studies of chalcone leading to 3-hydroxy-4,3',4',5'-tetramethoxychalcone and its analogues as potent nuclear factor κ B inhibitors and their anticancer activities. *J. Med. Chem.* **2009**, *52*, 7228–7235.
- (22) Milligan, D. W.; Grimwade, D.; Cullis, J. O.; Bond, L.; Swirsky, D.; Craddock, C.; Kell, J.; Homewood, J.; Campbell, K.; McGinley, S.; Wheatley, K.; Jackson, G. Guidelines on the management of acute myeloid leukaemia in adults. *Br. J. Haematol.* **2006**, *135*, 450–474.
- (23) Kurtova, A. V.; Balakrishnan, K.; Chen, R.; Ding, W.; Schnabl, S.; Quiroga, M. P.; Sivina, M.; Wierda, W. G.; Estrov, Z.; Keating, M. J.; Shehata, M.; Jager, U.; Gandhi, V.; Kay, N. E.; Plunkett, W.; Burger, J. A. Diverse marrow stromal cells protect CLL cells from spontaneous and drug-induced apoptosis: development of a reliable and reproducible system to assess stromal cell adhesion-mediated drug resistance. *Blood* **2009**, *114*, 4441–4450.
- (24) Stacchini, A.; Aragno, M.; Vallario, A.; Alfano, A.; Circo, P.; Gottardi, D.; Faldella, A.; Rege-Cambrin, G.; Thunberg, U.; Nilsson, K.; Caligaris-Cappio, F. MEC1 and MEC2: two new cell lines derived from B-chronic lymphocytic leukaemia in prolymphocytoid transformation. *Leuk. Res.* **1999**, *23*, 127–136.
- (25) Sambade, C.; Berglund, M.; Lagercrantz, S.; Sällström, J.; Reis, R. M.; Enblad, G.; Glimelius, B.; Sundström, C. U-2940, a human B-cell line derived from a diffuse large cell lymphoma sequential to Hodgkin lymphoma. *Int. J. Cancer* **2006**, *118*, 555–563.
- (26) Chang, H.; Blondal, J. A.; Benchimol, S.; Minden, M. D.; Messner, H. A. p53 mutations, c-myc and bcl-2 rearrangements in human non-Hodgkin's lymphoma cell lines. *Leuk. Lymphoma* **1995**, *19*, 165–171.
- (27) Tweeddale, M. E.; Lim, B.; Jamal, N.; Robinson, J.; Zalberg, J.; Lockwood, G.; Minden, M. D.; Messner, H. A. The presence of clonogenic cells in high-grade malignant lymphoma: a prognostic factor. *Blood* **1987**, *69*, 1307–1314.
- (28) Tweeddale, M.; Jamal, N.; Nguyen, A.; Wang, X. H.; Minden, M. D.; Messner, H. A. Production of growth factors by malignant lymphoma cell lines. *Blood* **1989**, *74*, 572–578.
- (29) Das, U.; Pati, H. N.; Panda, A. K.; De Clercq, E.; Balzarini, J.; Molnar, J.; Barath, Z.; Ocsovszki, I.; Kawase, M.; Zhou, L.; Sakagami, H.; Dimmock, J. R. 2-(3-Aryl-2-propenoyl)-3-methylquinoxaline-1,4-dioxides: a novel cluster of tumor-specific cytotoxins which reverse multidrug resistance. *Bioorg. Med. Chem.* **2009**, *17*, 3909–3915.
- (30) Dimmock, J. R.; Das, U.; Gul, H. I.; Kawase, M.; Sakagami, H.; Barath, Z.; Ocsovsky, I.; Molnar, J. 3-Arylidene-1-(4-nitrophenyl-methylene)-3,4-dihydro-1H-naphthalen-2-ones and related compounds displaying selective toxicity and reversal of multidrug resistance in neoplastic cells. *Bioorg. Med. Chem. Lett.* **2005**, *15*, 1633–1636.
- (31) Romagnoli, R.; Baraldi, P. G.; Carrion, M. D.; Cara, C. L.; Cruz-Lopez, O.; Preti, D.; Tolomeo, M.; Grimaudo, S.; Di Cristina, A.; Zonta, N.; Balzarini, J.; Brancale, A.; Sarkar, T.; Hamel, E. Design, synthesis, and biological evaluation of thiophene analogues of chalcones. *Bioorg. Med. Chem.* **2008**, *16*, 5367–5376.
- (32) Schobert, R.; Biersack, B.; Dietrich, A.; Knauer, S.; Zoldakova, M.; Fruehauf, A.; Mueller, T. Pt(II) complexes of a combretastatin A-4 analogous chalcone: effects of conjugation on cytotoxicity, tumor specificity, and long-term tumor growth suppression. *J. Med. Chem.* **2009**, *52*, 241–246.
- (33) Bellina, F.; Cauteruccio, S.; Monti, S.; Rossi, R. Novel imidazole-based combretastatin A-4 analogues: evaluation of their in vitro antitumor activity and molecular modeling study of their binding to the colchicine site of tubulin. *Bioorg. Med. Chem. Lett.* **2006**, *16*, 5757–5762.
- (34) Maioral, M. F.; Gaspar, P. C.; Rosa Souza, G. R.; Mascarello, A.; Chiaradia, L. D.; Licínio, M. A.; Moraes, A. C. R.; Yunes, R. A.; Nunes, R. J.; Santos-Silva, M. C. Apoptotic events induced by synthetic naphthylchalcones in human acute leukemia cell lines. *Biochimie* **2013**, *95*, 866–874.
- (35) Drexler, H. G. K-562. In *The Leukemia-Lymphoma Cell Line FactsBook*; Drexler, H. G., Ed.; Academic Press: London, 2001; pp 632–633.
- (36) Beesley, A. H.; Palmer, M. L.; Ford, J.; Weller, R. E.; Cummings, A. J.; Freitas, J. R.; Firth, M. J.; Perera, K. U.; de Klerk, N. H.; Kees, U. R. Authenticity and drug resistance in a panel of acute lymphoblastic leukaemia cell lines. *Br. J. Cancer* **2006**, *95*, 1537–1544.
- (37) Tang, R.; Faussat, A. M.; Perrot, J. Y.; Marjanovic, Z.; Cohen, S.; Storme, T.; Morjani, H.; Legrand, O.; Marie, J. P. Zosuquidar restores drug sensitivity in P-glycoprotein expressing acute myeloid leukemia (AML). *BMC Cancer* **2008**, *8*, 51.
- (38) Lubgan, D.; Jozwiak, Z.; Grabenbauer, G. G.; Distel, L. V. Doxorubicin-transferrin conjugate selectively overcomes multidrug resistance in leukaemia cells. *Cell. Mol. Biol. Lett.* **2009**, *14*, 113–127.
- (39) Parker, B. W.; Kaur, G.; Nieves-Neira, W.; Taimi, M.; Kohlhagen, G.; Shimizu, T.; Losiewicz, M. D.; Pommier, Y.; Sausville, E. A.; Senderowicz, A. M. Early induction of apoptosis in hematopoietic cell lines after exposure to flavopiridol. *Blood* **1998**, *91*, 458–465.
- (40) Dohse, M.; Scharenberg, C.; Shukla, S.; Robey, R. W.; Volkmann, T.; Deeken, J. F.; Brendel, C.; Ambudkar, S. V.; Neubauer, A.; Bates, S. E. Comparison of ATP-binding cassette transporter interactions with the tyrosine kinase inhibitors imatinib, nilotinib, and dasatinib. *Drug Metab. Dispos.* **2010**, *38*, 1371–1380.
- (41) Weisberg, E.; Manley, P. W.; Breitenstein, W.; Bruggen, J.; Cowan-Jacob, S. W.; Ray, A.; Huntly, B.; Fabbro, D.; Fendrich, G.; Hall-Meyers, E.; Kung, A. L.; Mestan, J.; Daley, G. Q.; Callahan, L.; Catley, L.; Cavazza, C.; Azam, M.; Neuberg, D.; Wright, R. D.; Gilliland, D. G.; Griffin, J. D. Characterization of AMN107, a selective inhibitor of native and mutant Bcr-Abl. *Cancer Cell* **2005**, *7*, 129–141.
- (42) Czyzewski, K.; Styczynski, J. Imatinib is a substrate for various multidrug resistance proteins. *Neoplasia* **2009**, *56*, 202–207.
- (43) Molica, S. Progress in the treatment of chronic lymphocytic leukemia: results of the German CLL8 trial. *Expert Rev. Anticancer Ther.* **2011**, *11*, 1333–1340.